Arch. Mech., 34, 5-6, pp. 581–592, Warszawa 1982

Turbulent flow behaviour through a shock wave
Turbulent macroscale evolution

J. F. DEBIEVE and D. BESTION (MARSEILLE)

THE PURPOSE of this study is to describe the behaviour of a turbulent field submitted to a shock wave. Experimental results concern velocity and temperature turbulent intensities as well as their time integral scales given by frequency analysis. Besides, classical relations between temperature and velocity fluctuations are examined in this nonequilibrium flow in terms of the fluctuation size. In this flow configuration with an energy supply at low frequency associated largely with production, we are led to formulate a linear type discontinuity model. When the mean flow characteristics are known, this model, built on the Reynolds tensor equation, allows to calculate the turbulent stresses evolution through the shock.

Praca dotyczy opisu zachowania się pola burzliwego w zetknięciu z falą uderzeniową. Prace doświadczalne dotyczą parametrów burzliwości prędkości i temperatury, jak również ich całek czasowych wynikających z analizy częstotliwości. Ponadto związki klasyczne między temperaturą i fluktuacjami prędkości badane są w tych przepływach nierównowagowych w zależności od wielkości fluktuacji. W takich przepływach, z dopływem energii przy niskich częstotliwościach związanym w głównej mierze z jej produkcją, dochodzimy do sformułowania modelu nieciągłości nieliniowego typu. Przy znanych średnich charakterystykach przepływu model ten, zbudowany na podstawie tensorowego równania Reynoldsa, pozwala obliczyć ewolucję naprężeń burzliwych na fali uderzeniowej.

Работа касается описания поведения турбулентного поля в столкновении с ударной волной. Экспериментальные работы касаются параметров турбулентности скорости и температуры, как тоже их временных интегралов, вытекающих из анализа частоты. Кроме этого классические соотношения между температурой и флуктуациями скорости исследуются в этих неравновесных течениях в зависимости от величины флуктуации. В таких течениях, с притоком энергии, при низких частотах, связанным в главной мере с ее производством, приходим к формулировке модели разрыва нелинейного типа. При известных средних характеристиках течения эта модель, построенная на основе тензорного уравнения Рейнольдса, позволяет рассчитать эволюцию турбулентных напряжений на ударной волне.

Introduction

SHOCK wave turbulence interaction raises the problem of understanding the behaviour of a turbulent field through a discontinuity. We shall examine a few analytical and experimental results concerning a shock wave-turbulent boundary layer interaction. An analysis was already proposed to calculate the Reynolds stress-tensor evolution through the shock [1]. We will add experimental results in order to study the validity of the hypothesis required to establish the model; more particularly, an experimental frequency analysis of the turbulent field will be carried out. The study of turbulent spectral distributions and their evolution gives qualitative information about the effects which play a leading part in the interaction. Moreover, time macro-scale data concerning some turbulent quantities will allow to quantify these effects.

1. Device and methods of measurement

A turbulent supersonic boundary layer on an adiabatic flat plate is deviated by a corner (6° deflection) without separation, (Fig. 1). The nominal Mach number is $M_\infty = 2.3$; the stagnation pressure is $P_i = 0.5$ atm, and the stagnation temperature is $\theta_{0i} = 293°K$. The boundary layer thickness is $\delta = 09.6$ mm upstream and $\delta = 9.25$ mm downstream; the corresponding Reynolds number based on the momentum thickness is $\mathscr{R}_\theta = 4.2 \cdot 10^3$ upstream.

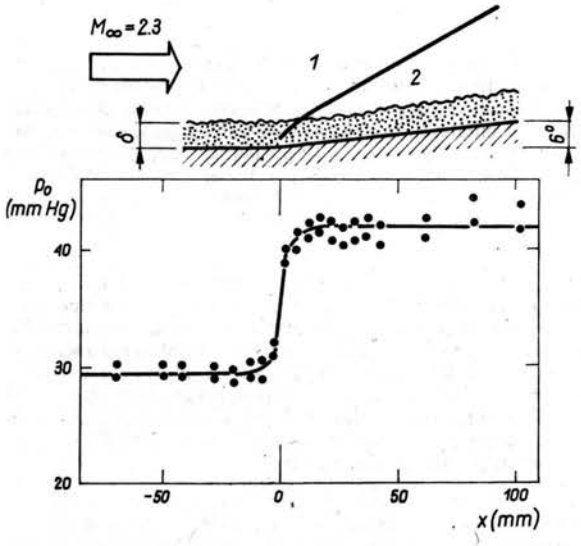

FIG. 1. Experimental arrangement. Wall pressure distribution.

Mean measurements are made using classical instruments. Turbulence measurements are performed using a constant current type hot wire anemometer; the 3 db frequency cut-off of the amplifier is 310 khz. Compensation of the thermal lag is electrically adjusted in situ and corrections for compensation circuit imperfections are applied (see [3] for the principle of the method). The wire is platinum-plated tungsten, the diameter and length of which are $\varnothing = 2.5\ \mu$ and $L = 0.7$ mm.

Hereafter, some indications about the method that provides spectral information are given. The electrical fluctuating voltage available at the output of the amplifier is applied to a spectrum analyser.

The energy representing signal plus noise is measured, as well as the noise level energy. The signal is a function of the stagnation temperature θ_0' and momentum $(\varrho U)'$ fluctuations. The spectral distributions of these quantities $\varphi_{\theta_0}(n)$ and $\varphi_{\varrho U}(n)$ are obtained using the fluctuation diagram method [4]. Velocity spectrum $\varphi_U(n)$, and temperature spectrum $\varphi_\theta(n)$ are deduced by assuming that the pressure fluctuation is negligible, as compared with the temperature fluctuation [4]. No correction is made concerning end loss effects which could modify the transfer function of the wire. The spectral decomposition method encounters many difficulties, so one may not expect a great accuracy of the absolute measured

values. Nevertheless, when the sources of errors are examined, we remark that they affect principally the absolute values: their evolution is altered, but to a lesser extent. As for the highest frequencies, these errors can become drastic, so that the only scales which have been significantly measured are greater than the Taylor's microscale.

2. Statement of the problem

As a rapid description of the mean flow, we will present a few important features. Values of the mean wall pressure data are given in Fig. 1. P_0 increases through the shock region ($\Delta P_0/P_0 \simeq 0.4$), over a longitudinal distance which, at the wall, is approximately equal to the boundary layer thickness δ. Consequently, the turbulent field is submitted to a strong deceleration over this distance. As an indication, mean velocity profiles upstream and downstream of the shock are given in Fig. 2. For further information see Ref. [2].

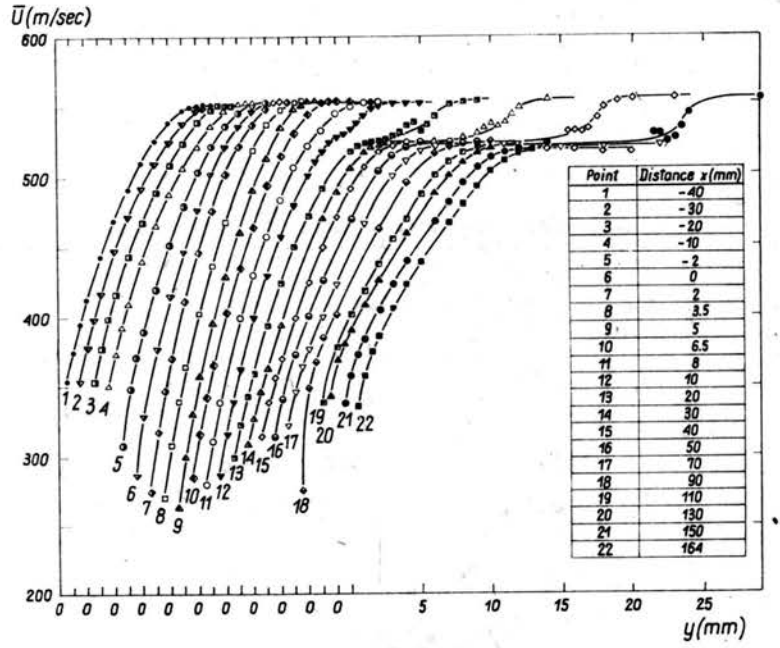

Point	Distance x(mm)
1	-40
2	-30
3	-20
4	-10
5	-2
6	0
7	2
8	3.5
9	5
10	6.5
11	8
12	10
13	20
14	30
15	40
16	50
17	70
18	90
19	110
20	130
21	150
22	164

FIG. 2. Mean velocity distribution.

This type of interaction where no separation is observed is characterized by the fact that the influence of turbulence on the mean flow is weak; the effect of the pressure forces is indeed more important than that of Reynolds stresses: the value of the classical ratio $\Delta p/\tau_0$ is $\simeq 60$.

This case is then particularly convenient to study the turbulent field distortion due to the strong mean gradients. Getting information about Reynolds stresses and turbulent

heat fluxes in this case can afford some advantages in order to study the effects of these terms in more complex interacting flows.

At the crossing of the shock, an increase of the velocity turbulence intensity is noticed.

This evolution is shown, along a mean streamline, in the middle of the boundary layer ($y/\delta = 0.4$), Fig. 3.

Analogous results may be observed in the greater part of the layer, (see Fig. 4 corresponding to sections on both sides of the shock). The tendency will be the same for the

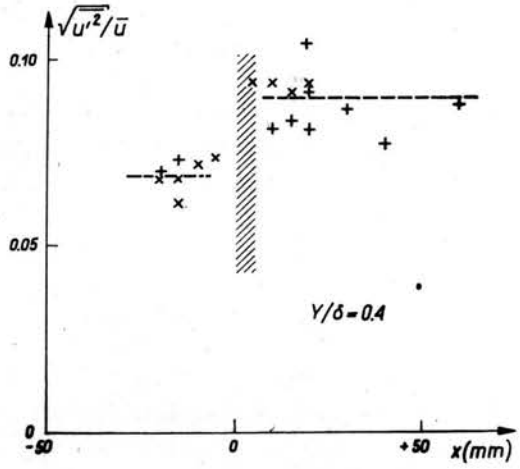

FIG. 3. Velocity turbulence intensity along a streamline.

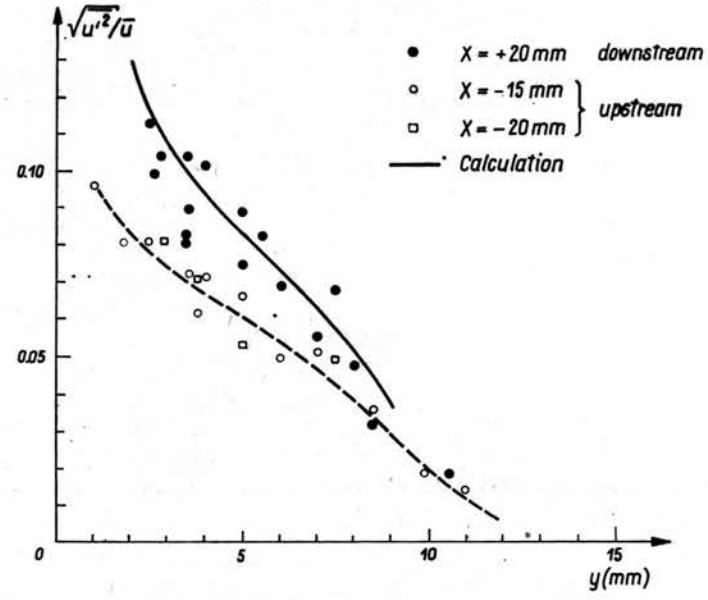

FIG. 4. Velocity turbulence intensity distribution upstream and downstream of the shock wave.

r.m.s. values $\sqrt{\overline{U'^2}}$. In the same way the temperature fluctuation r.m.s. value $\sqrt{\overline{\theta'^2}}$ increases through the shock but the turbulent intensity presents a much smaller evolution (Fig. 5).

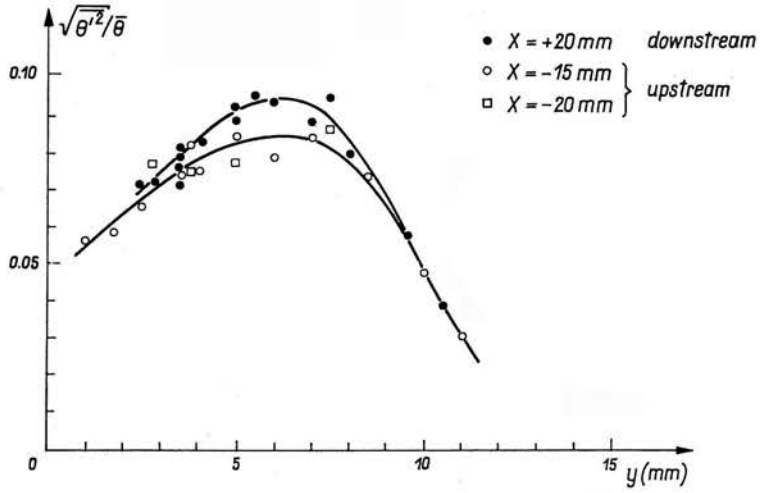

FIG. 5. Temperature turbulence intensity distribution upstream and downstream of the shock wave.

Classical relations between velocity and temperature fluctuations are now examined in such a distortion. The correlation coefficient $R_{u\theta}$ is measured on both sides of the shock. Figure 6 does not display any marked evolution for this correlation coefficient through the shock. In the same way the ratio $(\sqrt{\overline{\theta'^2}}/\overline{\theta})/(\gamma-1)M^2\sqrt{\overline{U'^2}}/\overline{U}$ between velocity and temperature turbulence intensity, which is approximately equal to 1, according to the strong Reynolds analogy relation, is not significantly changed by the interaction, (Fig. 7).

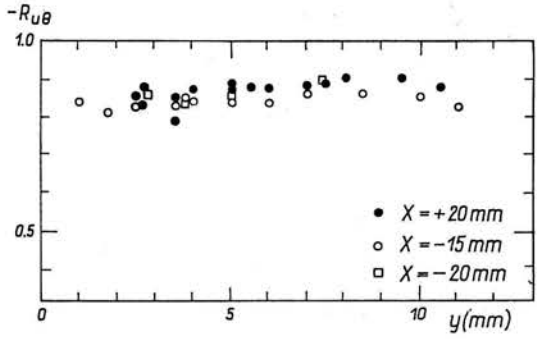

FIG. 6. Velocity temperature correlation coefficient distribution upstream and downstream of the shock.

3. Reynolds stress evolution analysis

The major part of the velocity turbulence level increase can be taken into account by an already proposed calculation which is hereafter summarized [1, 2]. Assumptions required for this calculation are derived from rapid distorsion theories [5, 6]. In order to

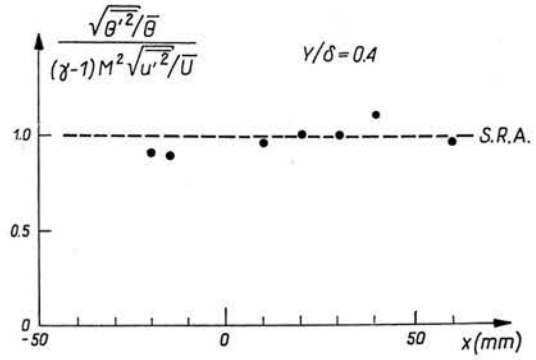

FIG. 7. "Strong Reynolds Analogy" relation along a stream-line through the shock.

test the consistency of the model, these assumptions led us to seek complementary experimental results on turbulent scales and their evolution. Since little information was found in the literature, other measurements were performed.

The starting point of the calculation is the Reynolds stress equation:

$$D_t\mathbf{T}+\{(\partial\tilde{\mathbf{U}}/\partial\mathbf{X})\mathbf{T}+\mathbf{T}(\partial\tilde{\mathbf{U}}/\partial\mathbf{X})^*\}=\mathbf{S},$$

where $\mathbf{T}=\overline{\varrho U'U'^*}/\bar{\varrho}$ is the matrix of Reynolds stresses; $\mathbf{S}$ corresponds to turbulent sources, other than kinetic production which belong to the left hand terms. As the flow is nearly discontinuous, it is convenient to write this equation in the Lagrangian form:

$$D_t\mathbf{T}_0=\mathbf{A}^*\mathbf{S}\mathbf{A} \quad \text{with} \quad \mathbf{T}_0=\mathbf{A}^*\mathbf{T}\mathbf{A}.$$

Let $\mathbf{T}_0$ be the tensor given by the linear tangential transformation A associated with the mean flow. $\mathbf{T}_0$ is an invariant for the operator corresponding to the transport and production terms. So it is much easier to take into account the discontinuity. We separate the mean deformation effect from the specific turbulent sources effect. These two equations equivalent to the Reynolds stress equation are extended to a discontinuity model, using a distribution formalism. So the downstream Reynolds tensor can be expressed, in terms of its upstream value and of the geometry and intensity of the shock, using a relation for which the realisability condition is fulfilled. The main hypothesis is the following one. Specific turbulent sources $\mathbf{S}$ are supposed to be weakly discontinuous: the discontinuity order is that of the Heaviside step, but it is not higher, [1]. Comparison between experimental results and calculation shows that most of the evolution is taken into account by the proposed analysis (Fig. 4). Indeed, the hypothesis was made a priori and cannot be directly justified. Consequently, new experiments are needed. More particularly, it is helpful to examine whether or not turbulent macro-scales and spectral distributions are coherent with the calculation scheme.

4. Frequency spectrum. Time macro-scale evolution

Frequency analysis of different fluctuating quantities gives some information about the frequency range containing energy. An evolution of the u' spectral distribution on both sides of the shock is given in Fig. 8. The measurements are carried out at two positions

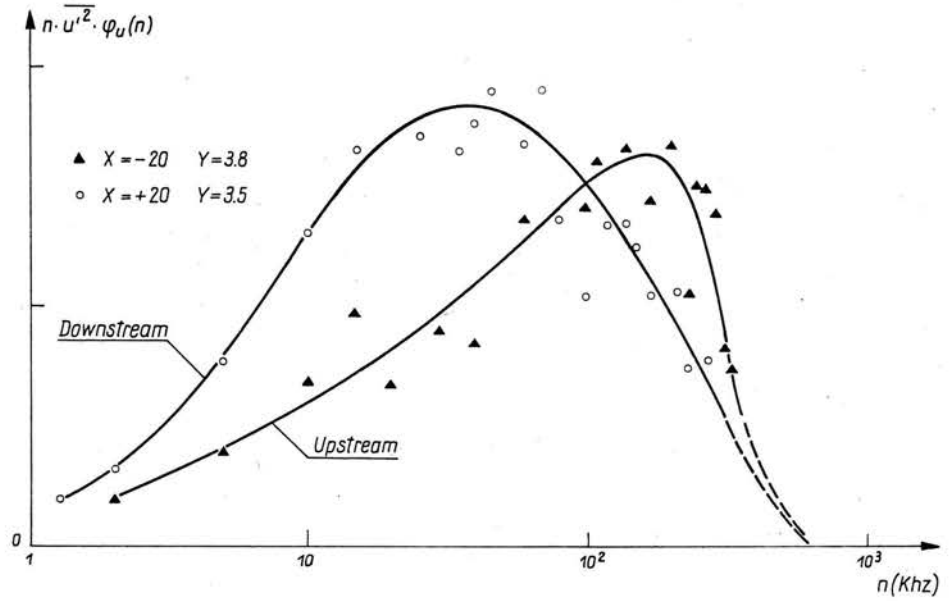

FIG. 8. Spectral velocity distribution, upstream and downstream.

of the same mean streamline in the representation $\overline{U'^2} n\varphi u(n)$ versus $\log n$, the frequency which corresponds to the maximum can be associated with a velocity time macro-scale.

An energy supply at low frequency is observed, which is here characterized by an increase of this time scale behind the shock. This result is completed by measurements performed: on the one hand along the streamline ($y/\delta \approx 0.4$), and on the other hand in two sections upstream and downstream of the shock. The spectrum shape evolution can also be characterized by the time integral scale

$$T_u = \varphi(0)/4 \quad \text{with} \quad \int_0^\infty \varphi(n)d = 1.$$

Figures 9 and 10 exhibit an increase of this integral scale T_u and this is true throughout the explored area of the boundary layer. A length scale can be deduced from this time scale by applying the Taylor's hypothesis: with the reservation due to the precision (see Sect. 1) one notes that, as in the case of the upstream boundary layer, the values of these length scales seem to be a bit smaller than in a subsonic case, when they are compared to the boundary layer thickness.

Keeping these results in mind, let us go back to the analysis. It is known that the linear terms of the Reynolds stress equation (particularly the production term which is very strong in the shock) induce an energy supply at low frequencies; such a mechanism would lead to the observed tendency. Besides, a rapid distortion criterion such as $\Lambda/q > \delta/U$ is verified when the turbulent characteristic time scale Λ/q is greater than the distortion time δ/u. This conditions is fulfilled in the interaction. Rapid distortion theories assume the existence of a relaxation time; this suggests that the turbulent sources terms S do not

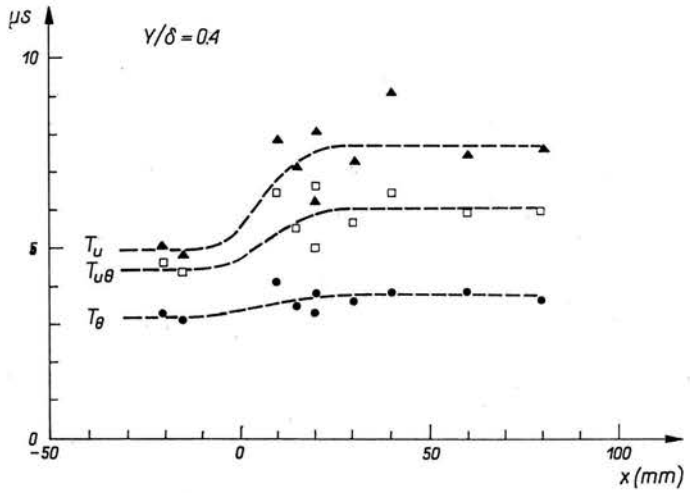

FIG. 9. Time integral macro-scales along a mean streamline.

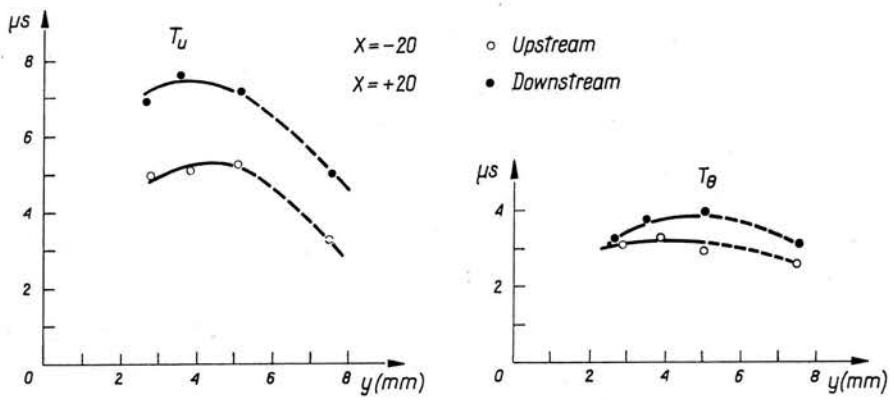

FIG. 10. Velocity and temperature time integral macro-scales distribution, upstream and downstream.

change too much through the interaction. It is consistent with the hypothesis which we used in the scheme concerning the weak discontinuity of the sources **S** (Sect. 3).

After these considerations about turbulent momentum fluxes, we precise now the behaviour of the turbulent heat field. First we shall examine the thermal scale and its evolution. Then, changes in the relations between temperature and velocity fields will be studied in terms of the fluctuation "size".

It appears in Figs. 8 and 11 that the frequency ranges concerned with temperature and velocity do not differ very much from each other. As in the case dealing with the velocity field, temperature spectrum downstream of the shock displays a small displacement of energy towards lower frequencies when compared to the upstream spectrum; but the phenomenon is less marked than for the velocity case.

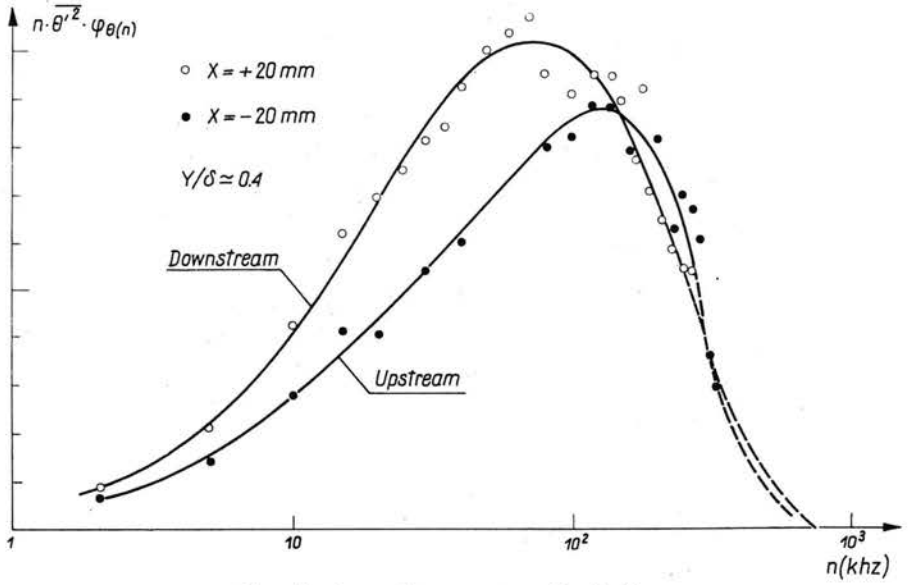

FIG. 11. Spectral temperature distribution.

This tendency is confirmed by the small increase of the temperature time integral scale observed in Figs. 9 and 10.

As an indication, we also give the time integral scale evolution concerning mixed quantities compound with velocity and temperature:

the velocity-temperature correlation integral scale $U_{u\theta}$ associated to the cospectrum $\varphi_{u\theta}(n)$ (Fig. 9),

the stagnation temperature scale T_{θ_0} (Fig. 12),

the momentum scale $T_{\varrho u}$ (Fig. 12).

Frequency analysis of the temperature-velocity correlation coefficient is presented in Fig. 13. This coefficient seems to be constant in the greater part of the frequency range,

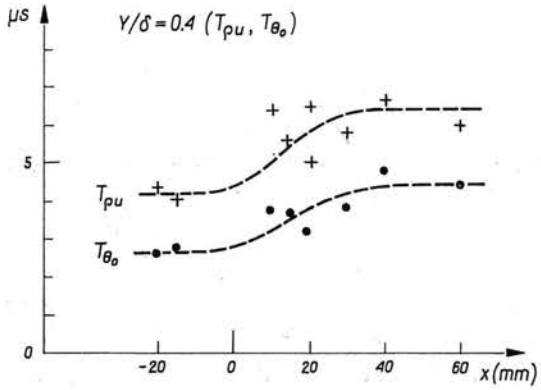

FIG. 12. Stagnation temperature and momentum integral macro-scales.

except for very low frequencies. Moreover, this pattern is not altered through the shock. The ratio $\frac{\bar{u}[\overline{\theta'^2}\cdot\varphi_\theta(n)]^{1/2}}{(\gamma-1)M^2\bar{\theta}[\overline{u'^2}\varphi_u(n)]^{1/2}}$ which expresses the Strong Reynolds Analogy relation at each frequency is plotted in Fig. 14. Departures from the analogy do not present exactly the same frequency distribution upstream and downstream of the shock, although the SRA relation concerning the unfiltered quantities is nearly verified everywhere. The ratio between temperature and velocity integral scales is changed through the shock (Fig. 15).

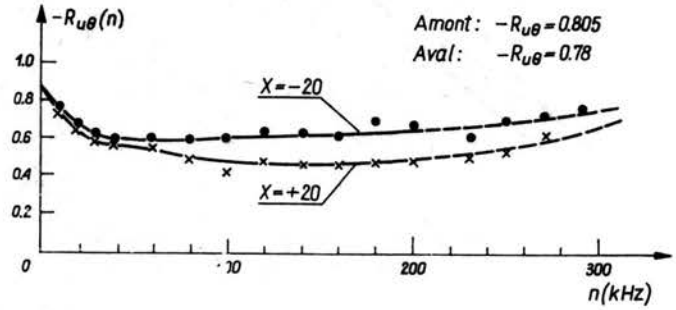

FIG. 13. Spectral distribution of the velocity temperature correlation coefficient.

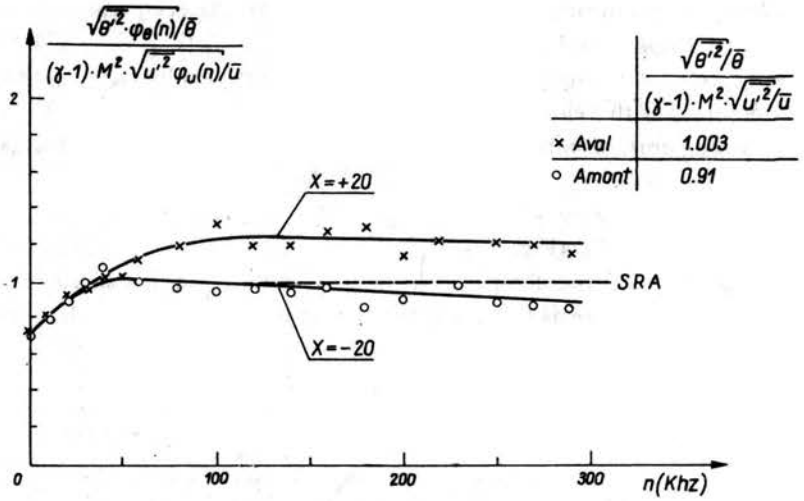

FIG. 14. Spectral distribution of the "Strong Reynolds Analogy" relation.

Another interesting feature is available in these measurements: it concerns the evolution of the stagnation temperature field. In fact, this physical quantity is a combination of the velocity and temperature fluctuation and the results concerning this quantity correspond to another presentation of the relation between temperature and velocity. First we remark that the mean stagnation temperature $\bar{\theta}_0$ remains practically constant through the shock. Moreover, no significant evolution of the turbulence intensity $\sqrt{\overline{\theta_0'^2}}/\bar{\theta}_0$ is ob-

served (Fig. 16) in the interaction. Considering the following equation concerning the evolution of $\frac{\overline{\varrho\theta_0'^2}}{\bar{\varrho}} \simeq \overline{\theta_0'^2}$

$$\underbrace{D_t \frac{\overline{\varrho\theta_0'^2}}{\bar{\varrho}}}_{} = \underbrace{-2\frac{\overline{\varrho u_k' \theta_0'}}{\bar{\varrho}} \partial_k \tilde{\theta}_0}_{\text{Production}} \underbrace{- \frac{1}{\varrho}\overline{\partial_k(\varrho u_k' \theta_0'^2)} + \frac{2}{\bar{\varrho}\bar{C}_p}\overline{\theta_0' \partial_t p} + \frac{2}{\bar{\varrho}\bar{C}_p}\overline{\theta_0' \partial_k(f_{ik}u_i - h_k)}}_{\text{Sources}},$$

we first look after the terms which can play a leading part and which involve strong mean gradients due to the shock. The only term which is explicitly formed with a mean gradient is the production term. The gradient $\partial_k \tilde{\theta}_0$ is practically unchanged by the shock, so it cannot contribute to a step of $\overline{\varrho\theta'^2}/\bar{p}$.

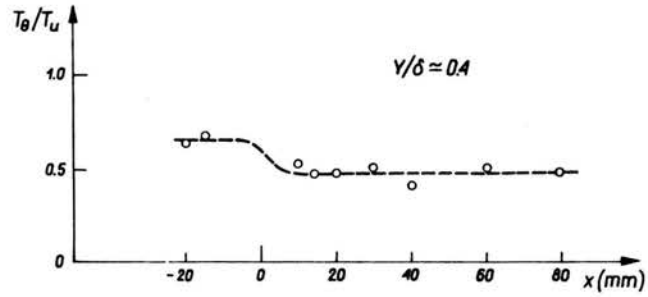

FIG. 15. Ratio of the velocity and temperature integral macro-scales.

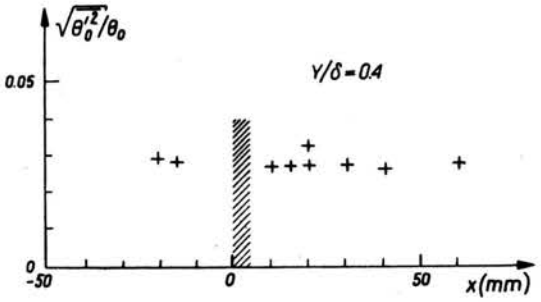

FIG. 16. Stagnation temperature turbulence intensity along a streamline.

Therefore, these considerations about thermal quantities state the connections with the dynamical turbulent field about which spectral analysis showed that "linear effects" play a leading part.

References

1. J. F. DEBIEVE, *Bilan des tensions de Reynolds dans une interaction onde de choc-turbulence*, C. R. Acad. SC., Serie BT. 291, 1980.
2. J. F. DEBIEVE, H. GOUIN, J. GAVIGLIO, *Momentum and temperature fluxes in a shock wave-turbulence interaction*, ICHMT/IUTAM 1980 Symposium on the Structure of Turbulence and Heat and Mass Transfer; Hemisphere Publishing Corporation, Dubrovnik 1980.

3. J. GAVIGLIO, *Sur les methodes de l'anemometrie par fil chaud des écoulements turbulents compressibles de gaz*, J. de Meca. Appl., **2**, 4, 449, 1978.
4. J. F. DEBIEVE, D. BESTION, *Interaction onde de choc-ecoulement cisaillé, Evolution des tensions de Reynolds*, R.T.O.N.E.R.A. 21/1455 AN, 1980.
5. G. K. BATCHELOR, I. PROUDMAN, *The effect of rapid distorsion of a fluid in turbulent motion*, Quart. Journ. Mech. and Appl. Math. part 1, **7**, 1954.
6. J. P. DUSSAUGE, J. F. DEBIEVE, *Influence d'un fort gradient de pression sur des perturbations instationnaire de vitesse*, 15e Colloque d'Aerodynamique Appliquée, A.A.A.F., Marseille 1978.

INSTITUT DE MECANIQUE STATISTIQUE DE LA TURBULENCE, MARSEILLE

and

OFFICE NATIONAL d'ETUDE ET DE RECHERCHES AEROSPATIALES
CHATILLON—SOUS—BAGNEUX, FRANCE.

Received November 9, 1981.